Gas Transport and Ionic Transport in Membranes Based on Polynorbornenes with Functionalized Imide Side Groups

Joel Vargas, Arlette A. Santiago, and Mikhail A. Tlenkopatchev

Instituto de Investigaciones en Materiales, Universidad Nacional Autónoma de México, Apartado Postal 70-360 CU, Coyoacán, México DF 04510, México

Rubén Gaviño

Instituto de Química, Universidad Nacional Autónoma de México, CU, Coyoacán, México DF 04510, México

Maria Fe Laguna, Mar López-González, and Evaristo Riande*

Instituto de Ciencia y Tecnología de Polímeros (CSIC), 28006 Madrid, Spain

Received October 31, 2006; Revised Manuscript Received November 21, 2006

ABSTRACT: This work reports the synthesis and hydrogenation of polynorbornenes with functionalized imide side groups, specifically, poly(*N*-phenyl-*exo,endo*-norbornene-5,6-dicarboximide), as well as the sulfonation of the hydrogenated polymer. The gas transport characteristics and permselectivity of membranes prepared from the three separated polymers were thoroughly investigated. The results show that hydrogenation of the starting polymer promotes packaging efficiency, which is even enhanced by further sulfonation of the hydrogenated chains. The economy of free volume is reflected in the permeation and permselectivity coefficients of membranes prepared from the polymers. The study of electromotive forces of concentration cells with the sulfonated membrane separating hydrochloric solutions of different concentration suggests that the membranes exhibit high permselectivity to protons that decreases as concentration increases. However, a sharp increase in the electromotive force occurs at high concentrations. The fact that this increase is not observed in the electromotive forces of concentration cells with sodium chloride in the compartment cells suggests the formation of pair ions between protonated imide groups and chloride ions at high concentration that restrains co-ions mobility in the membrane. The membranes exhibit pretty good permselectivity to protons and sodium ions which makes them useful for ionic separation applications, such as electrodialysis. However, owing to the low water uptake, the protonic conductivity of the membranes equilibrated with water is nearly 2 orders of magnitude below that reported for Nafion membranes.

Introduction

The participation of membranes technology in industrial gas separation processes is ever-growing in the past decades.[1] Gas transport across membranes under a negative unidirectional driving force perpendicular to the membrane involves solution of the gas in the membrane, diffusion across the membrane, and desorption at the other side of the membrane. Obviously, these processes depend on the state (glassy, rubbery, or semicrystalline) of the membrane. Either sorption, diffusion, or both may control gas permselectivity in glassy membranes while solubility is the only factor controlling this property in rubbery membranes. Great efforts are being made in the development of membranes exhibiting high selectivity combined with high permeability. Polymeric materials with bulky groups in their structures may contain high size cavities that facilitate gas diffusion without affecting very negatively gas permselectivity. Development of membranes based on materials of this type has focused the attention of many researchers in the past decades.[2]

Owing to the facile functionalization and high ring-opening methathesis polymerization (ROMP) reactivity of norbornene monomers,[3,4] polymers with different structures can be derived from functionalized norbornenes that can be useful for the development of membranes for gas separation. The capability of polynorbornenes for packaging and gas separation processes has been investigated.[5−9] Gas transport studies in ring preserved polynorbornenes prepared via addition polymerization have also been reported.[10,11] The double bonds of the main chain of polynorbornenes confer rigidity to the molecular chains, thus hindering molecular packaging. Earlier work[12−14] has shown that the permeability coefficient of oxygen across membranes of polynorbonenes with functionalized imide side groups is nearly 5 times that of nitrogen. Also, these membranes may exhibit much higher permselectivity than the membranes prepared from poly(trimethylsilylnorbornene) and fluorine-containing ring-opened polynorbornenes.[6,7] With the aim of investigating the effect of the increase of conformational versatility of the chains on gas permselectivity, poly(*N*-phenyl-*exo,endo*-norbornene-5,6-dicarboximide) (Poly-PhNDI) was hydrogenated, and membranes were prepared from the resulting polymer, Poly-HPhNDI. It is expected that the increase in chain flexibility of Poly-HPhNDI promoted by the hydrogenation of the double bonds of Poly-PhNDI facilitates molecular packaging. At first glance this effect will decrease gas permeability, and as a result one would expect that gas permselectivity is also enhanced. Therefore, this work reports gas transport across membranes of Poly-HPhNDI, and the results obtained are compared with those found for membranes of Poly-PhNDI.

The development of new polyelectrolytes has become a flourishing field of research because, aside from their traditional use in ionic separation processes, cation-exchange membranes are being investigated as electrolytes for batteries and fuel cells.[15] Also, a wealth of information concerning gas transport

‡ Corresponding author. E-mail: riande@ictp.csic.es.

10.1021/ma062522q CCC: $37.00
Published on Web 01/06/2007

in ion-exchange membranes is available. For example, the combination of permeability and ideal selectivity for O_2/N_2 and CO_2/CH_4 places sulfonated poly(phenyl oxide) membranes below the respective upper bound lines for polymeric membranes.[16] However, an increase in the ion-exchange capacity brings the ideal selectivity vs permeability relationship closer to the upper bound line, especially for the O_2/N_2 gas pair. Gas transport facilitated can be used to separate alkanes from alkenes.[17] The separation factor for ethylene/ethane across membranes prepared from blends of silver (I)-form Nafion and 2% of poly(pyrrole) increases from 8 to 15 as temperature decreases.[18] The facilitated transport model for CO_2 through ion-exchange membranes containing a diamine complexing agent was also reported. The diamine behaves as a mobile carrier for carbon dioxide.[19] In view of these preceding facts, one of the purposes of this work was to examine the effect of sulfonation on the gas transport properties and permselectivity of Poly-HPhNDI membranes. To accomplish this goal, we have undertaken the sulfonation of Poly-HPhNDI with acetylsulfonic acid. Sulfonation of the double bonds of polynorbornenes has already been described.[20,21] In this work, however, sulfonation was not carried out in the main chain, but in the phenyl group attached to the imide group. Membranes were prepared by casting from this polyelectroyte solutions, and their gas transport characteristics were investigated.

As a natural extension of the studies of the gas transport characteristics of sulfonated Poly-HPhNDI, we have also investigated the ionic permselectivity of these membranes. To accomplish this goal, the electromotive forces of the concentration potential cells of sulfonated Poly-HPhNDI membranes were measured keeping the ratio between the concentrations of the concentrated and dilute compartments in the vicinity of two. As polyelectrolytes, sodium chloride solutions and hydrochloric acid were used. From the electromotive forces the counterion transport numbers were obtained, and the effect of the concentration of the electrolyte solutions on the counterion transport number was investigated. Information concerning the diffusion of protons in the sulfonated membrane equilibrated with water was also obtained from the proton conductivity measured at room temperature.

Experimental Section

Materials. *Exo* (90%)- and *endo* (10%)-norbornene-5,6-dicarboxylic anhydride (NDA) was prepared via Diels−Alder condensation of cyclopentadiene and maleic anhydride. Maleic anhydride (18 g, 0.18 mol) was dissolved in 60 mL of trichlorobencene and heated at 190 °C. An amount of 12 g (0.09 mol) of dicyclopentadiene was added dropwise to the stirred solution of maleic anhydride. The reaction was maintained at 190 °C for 3 h and then cooled. The mixture was precipitated in 200 mL of hexane. The obtained solid was filtered, washed several times with hexane, and dried in a vacuum oven at 50 °C overnight. NDA was obtained after three recrystallizations from toluene: yield = 70%; mp = 102−104 °C. Aniline, acetic anhydride, sulfuric acid, and other chemicals were purchased from Aldrich Chemical Co. 1,2-Dichloroethane, dichloromethane, *p*-dioxane, and toluene were dried over anhydrous calcium chloride and distilled over CaH_2. 1,3-Bis(2,4,6-trimethylphenyl)-4,5-dihydroimidazol-2-ylidene)$(PCy_3)Cl_2Ru$=CHPh and $ClRh(PPh_3)_3$ were purchased from Aldrich Chemical Co. and used as received.

Characterization. ^{1}H NMR and ^{13}C NMR spectra were recorded with a Varian spectrometer at 300 and 75.5 MHz, respectively, in $CDCl_3$ using tetramethylsilane (TMS) as internal standard.

The glass transition temperature was measured with a DuPont 2100 instrument at a heating rate of 10 °C/min. The samples were encapsulated in standard aluminum DSC pans in duplicate. Each pan was run twice on the temperature range 30−300 °C. FTIR spectra were obtained on a Nicolet 510 p spectrometer. Molecular weights and molecular weight distributions with reference to polystyrene standards were determined on a Varian 9012 GPC instrument at 30 °C in chloroform (universal column and a flow rate of 1 mL min^{-1}).

Scheme 1. Synthesis of *N*-Phenyl-*exo*,*endo*-norbornene-5,6-dicarboximide (PhNDI, 2)

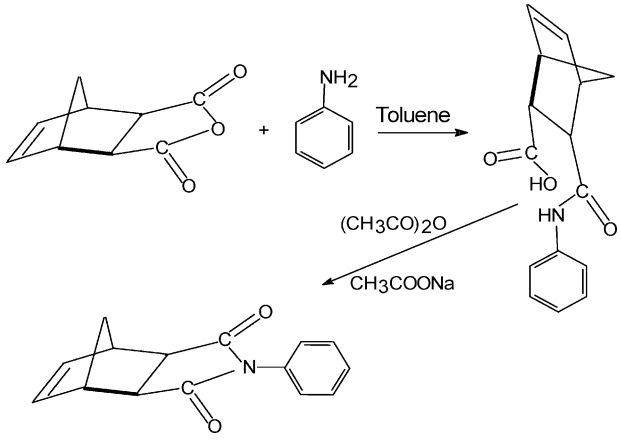

Monomer Synthesis. *N*-Phenyl-*exo*,*endo*-norbornene-5,6-dicarboximide (PhNDI, **2**) was synthesized according to literature (Scheme 1).[12,22] NDA (5 g, 30.5 mmol) was dissolved in 50 mL of toluene. An amount of 2.8 g (30.1 mmol) of aniline in 10 mL of toluene was added dropwise to the stirred solution of NDA. The reaction was maintained at 50 °C for 3 h. A precipitate was filtered and dried to give 7.6 g (29.5 mmol) of amic acid **1**. The amic acid obtained (7.6 g, 29.5 mmol), anhydrous sodium acetate (3.0 g, 36 mmol), and acetic anhydride (21 g, 212 mmol) were heated at 90 °C for 6 h and then cooled. The solid crystallized on cooling was filtered, washed several times with water, and dried in a vacuum oven at 50 °C overnight. Pure monomer **2** was obtained after twice recrystallization from toluene: yield = 81%; mp = 195−196 °C. ^{1}H NMR (300 MHz, $CDCl_3$) (Figure 1): δ (ppm) = 7.49−7.25 (5H, m), 6.33 (2H, s), 6.24 (2H, s), 3.38 (2H, s), 2.84 (2H, s), 1.62−1.46 (2H, m). ^{13}C NMR (75 MHz, $CDCl_3$): δ (ppm) = 176.8 (C=O), 137.8 (C=C), 134.4, 131.7 (C−N), 129.0, 128.4, 126.2, 47.7, 45,7, 42.8. FT-IR: 3064 (C=C−H str), 2946 (C−H asym str), 2877 (C−H sym str), 1770 (C=O), 1594 (C=C str), 1454 (C−N), 1382, 1329, 1289, 1188, 975, 799 cm^{-1}.

Monomer Metathesis Polymerization. Ring-opening metathesis polymerizations were carried out in glass vials under a dry nitrogen atmosphere at room temperature. Adding ethyl vinyl ether under a dry nitrogen atmosphere terminated the reactions. After cooling, the solutions were poured into an excess of methanol. The polymer was purified by solubilizing into chloroform containing a few drops of 1 N HCl and precipitating into methanol. The obtained polymer was dried in a vacuum oven at 40 °C to constant weight.

Polymer Synthesis. Poly(*N*-phenyl-*exo*,*endo*-norbornene-5,6-dicarboximide) (Poly-PhNDI, **3**). 1 g (4.18 mmol) of **2** and 0.0035 g (0.0041 mmol) of catalyst **I** were stirred in 6.0 mL of 1,2-dichloroethane at room temperature for 1 h (Scheme 2). The obtained polymer **3** was soluble in chloroform and dichloromethane. ^{1}H NMR (300 MHz, $CDCl_3$) (Figure 1): δ (ppm) = 7.42−7.21 (5H, m), 5.78 (2H, *trans*, s), 5.54 (2H, *cis*, s), 3.49 (2H, s), 3.14−2.86 (2H, m), 2.16 (1H, s), 1.61 (1H, s). ^{13}C NMR (75 MHz, $CDCl_3$): δ (ppm) = 177.1, 133.7 (*cis*), 131.8 (*trans*), 128.9, 126.3, 52.5, 50.9, 48.6, 46,0, 42.8, 40.5. FT-IR: 3034 (C=C−H ar str), 2930 (C−H asym str), 2869 (C−H sym str), 1775 (C=O), 1590 (C=C str), 1457 (C−N), 1385, 1323, 1290, 1165, 980, 790 cm^{-1}. The values of the number-average molecular weight, M_n, polydispersity, M_w/M_n, glass transition (T_g), and decomposition (T_d) temperature of poly(*N*-phenyl-*exo*,*endo*-norbornene-5,6-dicarboximide were respectively $M_n = 2.1 \times 10^5$, $M_w/M_n = 1.3$, $T_g = 222$ °C, and $T_d = 418$ °C.

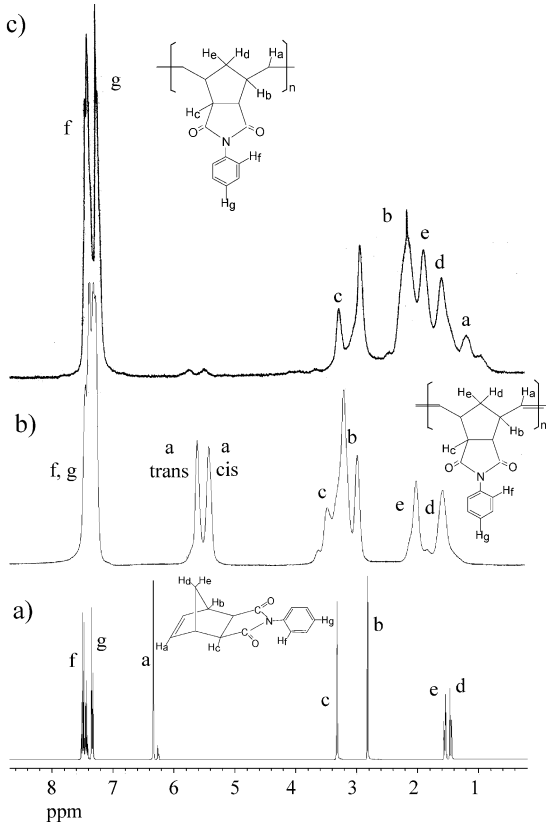

Figure 1. ^{1}H NMR spectra of (a) monomer **2**, (b) polymer **3**, and (c) its saturated analogue, polymer **4**.

Scheme 2. Ring-Opening Metathesis Polymerization of *N*-Phenyl-*exo,endo*-norbornene-5,6-dicarboximide (PhNDI, 2)

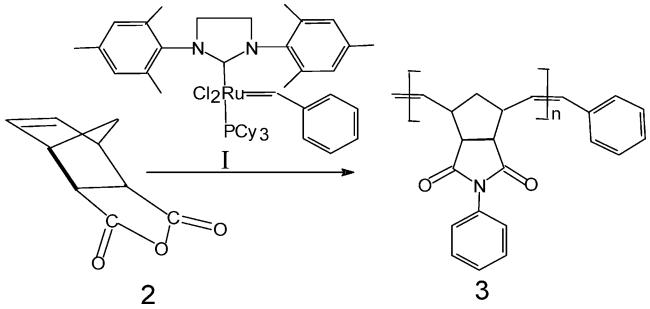

Scheme 3. Hydrogenation of Poly(*N*-phenyl-*exo,endo*-norbornene-5,6-dicarboximide) (Poly-PhNDI, 3) by Wilkinson's Catalyst

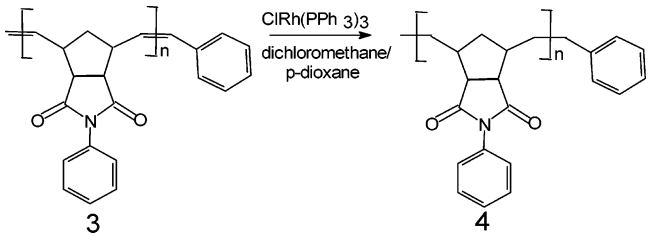

Polymer Hydrogenation. The hydrogenation of poly(*N*-phenyl-*exo,endo*-norbornene-5,6-dicarboximide) (Poly-PhNDI, **3**) (Scheme 3) was made using several catalysts. The reaction was investigated at room temperature and pressures ranging from 1 to 115 bar. The catalysts employed in the reaction were Pd/C, PtO_2, Al/Ni, and Wilkinson catalyst $ClRh(PPh_3)_3$.

A Parr shaker hydrogenator was used. This apparatus provides compact and easily operated systems for the treatment of chemicals with hydrogen in the presence of a catalyst at pressure up to 5 bar. The polymer to be treated in a Parr hydrogenator is sealed in a reaction bottle with the catalyst and connected to a hydrogen reservoir. Air is removed by evacuating the bottle. Pressure is then applied from the reservoir, and the bottle is shaken vigorously to initiate the reaction. The progress of the reaction was followed by observing the pressure drop in the system and by ^{1}H NMR (Figure 1). The reaction at high pressure was carried out in a stainless steel 160 mL autoclave (Parr).

Scheme 4. Sulfonation of Hydrogenated Poly(*N*-phenyl-*exo,endo*-norbornene-5,6-dicarboximide) (Poly-HPhNDI, 4)

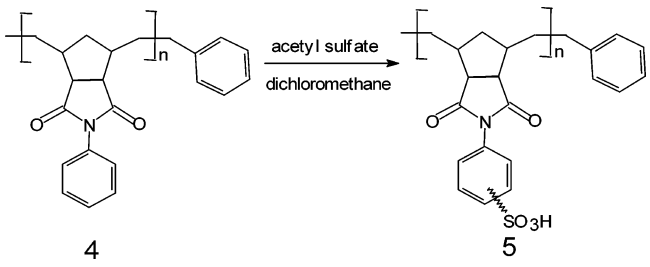

^{1}H NMR spectra of hydrogenated polymer (Poly-HPhNDI, **4**) were obtained on a Varian Gemini spectrometer at an observation frequency of 200 MHz with TMS as internal standard.

In a typical procedure, 0.5 g of Poly-PhNDI (**3**) was added to 60 mL of solvent in a Schlenk tube. The catalyst (5 wt %) was previously introduced into the reactor. The solution was degassed and charged into the reactor under N_2. Hydrogen was added.

Experiments were carried out using several solvents, and the mixture dichloromethane−*p*-dioxane (1:1) provided the best result.

The hydrogenation level was determined by integrating the area, in the ^{1}H NMR spectrum, of the olefinic proton region ($\delta = 5-6$ ppm) relative to aromatic proton region ($\delta = 7-8$ ppm) (Figure 1). A 99% of hydrogenation for Poly-PhNDI (**3**) was achieved by Wilkinson catalyst $ClRh(PPh_3)_3$ at room temperature and 115 bar. ^{1}H NMR (300 MHz, $CDCl_3$) (Figure 1): δ (ppm) = 7.42−7.21 (5H, m), 3.34 (2H, s), 2.92 (2H, s), 2.21 (2H, s), 1.98 (1H, s), 1.61 (1H, s), 1.25 (2H, s). FT-IR: 3028 (C═C−H ar str), 2931 (C−H asym str), 2870 (C−H sym str), 1780 (C═O), 1459 (C−N), 1382, 1324, 1291, 1164, 982, 793 cm^{-1}. The values of the number-average molecular weight, M_n, polydispersity, M_w/M_n, glass transition (T_g), and decomposition (T_d) temperature of hydrogenated poly(*N*-phenyl-*exo,endo*-norbornene-5,6-dicarboximide) were respectively $M_n = 2.3 \times 10^5$, $M_w/M_n = 1.6$, $T_g = 197$ °C, and $T_d = 460$ °C.

Polymer Sulfonation. Prior to the polymer sulfonation, acetyl sulfate was prepared, according to literature,[23] by cooling 5 mL of dichloromethane in an ice bath for 10 min. Under stirring conditions, 0.7 mL of acetic anhydride and 0.3 mL of sulfuric acid were added to the chilled dichloromethane. The latter was added 10 min after the addition of the former.

In a typical sulfonation procedure, 1.0 g of hydrogenated polymer (Poly-HPhNDI, **4**) was dissolved in 20 mL of dichloromethane and purged with nitrogen. The 5% (w/v) polymer solution was stirred at room temperature. Then, 6.0 mL of acetyl sulfate solution, prepared as described above, was slowly added to begin the sulfonation reaction. The reaction was terminated after 18 h by precipitating in 50 mL of methanol. The precipitate was washed several times with deionized water. The obtained polymer (Scheme 4) was then dried in a vacuum oven at 50 °C for 24 h. The product was characterized by FT-IR and elemental analysis. The sulfonated Poly-HPhNDI was soluble in most common organic solvents such as dimethyl sulfoxide, dimethylformamide, and *N*,*N*-dimethylacetamide, among others. Sulfonation degree was $DS_T = 0.40$ (calculated by titration) and $DS_{EA} = 0.36$ (calculated by elemental analysis). $C_{15}H_{13}O_5NS$ (319): Calcd C 56.42, H 4.07, O 25.07, N 4.38, S 10.03; Found C 65.89, H 6.02, O 19.33, N 5.06, S 3.68. $T_{d1} = 313$ °C (sulfonic group loss); $T_{d2} = 440$ °C (main chain decomposition). The T_g of sulfonated polymer **5** is much higher than that of its parent poly-HPhNDI ($T_g = 197$ °C), and no T_g was detectable for **5** before its thermal decomposition. FT-IR: 3042 (C═C−H ar str), 2950 (C−H asym str), 2887 (C−H sym str), 1800

(C=O), 1450 (C−N), 1370, 1160, 1093 (−SO_3H, asym str), 1025 (−SO_3H, sym str), 730 cm^{-1}.

Gas Permeation. Gas transport was measured in an experimental device made of two compartments separated by the membrane. Vacuum was made in the two compartments, and gas stored in a reservoir in the vicinity of the pressure of interest was allowed to flow into one of the compartments called hereafter upstream chamber. The flow of gas from the upstream chamber to the low pressure or downstream chamber was monitored with a MKS-722 (0−10 Torr) pressure sensor via a PC. The pressure in the upstream chamber was measured with a Gometrics (0−10 bar) pressure sensor. The gas permeation apparatus was immersed in a water thermostat.

Water Uptake and Ion-Exchange Capacity. Weighed dry membranes were immersed and kept in deionized distilled water overnight. The membranes were removed from water, gently blotted with filter paper to remove surface water, and weighed. This operation was repeated three times. Water uptake was obtained by means of the expression

$$\text{water uptake} = \frac{\text{weight wet membrane} - \text{weight dry membrane}}{\text{weight dry membrane}} \times 100 \quad (1)$$

To evaluate the ion-exchange capacity, the membranes in the acid form were equilibrated with a NaCl solution (1 M), and the hydrochloric acid liberated in the interchange reaction

$$R{-}H + Na^+ \rightarrow R{-}Na + H^+$$

was titrated with a 0.01 M sodium hydroxide solution. The values of the ion-exchange capacity and the water uptake are respectively 0.82 mequiv/g dry membrane and 12.4%.

Electromotive Force of Concentration Cells. The electromotive force of the concentration cell with configuration Ag|AgCl|electrolyte concentration (m_1)|cation-exchange membrane|electrolyte concentration (m_2)|AgCl|Ag, where m represents the molal concentration, was measured with a Hioki potentiometer, at 25 °C, for various concentrations of both hydrochloric acid and sodium chloride solutions. Electromotive forces were monitored as a function of time via a PC. The ratio of the molal concentrations m_2/m_1 was kept in the vicinity of 2 in all the cases.

Ionic Conductivity of the Cation-Exchange Membranes. The resistance of the membranes equilibrated with distilled water, R_0, was measured by impedance spectroscopy over the frequency window 10^6-10^9 Hz, with a Novocontrol (Huntsangen, Germany) system using a HP4291 (Hewlett-Packard, Hyogo, Japan) coaxial line refractometry. The complex impedance was determined by measuring the reflection coefficient at a particular reference plane.[24] The protonic resistance, R_0, was obtained from the Bode diagram[25] as the modulus of the complex impedance in the plateau of high-frequency region at which $\varphi = \tan^{-1}(Z''/Z') = 0$. The measurements were carried out at 25 °C. The conductivity of the membranes was obtained from

$$\sigma = \frac{l}{R_0 A} \quad (2)$$

where A and l are respectively the area and thickness of the membranes sandwiched between the electrodes.

Results

(A) Gas Permeation. As usual, the curves describing gas permeation across membranes were monitored measuring the evolution of the pressure in the downstream chamber with time. The isotherms present a transitory transport process followed by a linear dependence of pressure on time that reflects gas flow under steady-state conditions. The permeability coefficient, P, was obtained from the slope of the straight line of the p vs t plot by means of the expression

$$P = \frac{273}{76}\frac{Vl}{p_0 TA}\lim_{t\to\infty}\frac{dp}{dt} \quad (3)$$

where p_0 is the pressure in the upstream chamber, V is the volume of the downstream chamber, T is the absolute temperature, and l and A are respectively the thickness and permeation area of the membrane. Usually P is given in barrers [1 barrer $= 10^{-10}$ cm^3 (STP) cm/(cm^2 s cmHg)]. The diffusion coefficient was obtained from time-lag θ that corresponds to the intersect of the straight line p vs t with the abscissa axis, using the equation suggested by Barrer[26]

$$D = \frac{l^2}{6\theta} \quad (4)$$

Usually D is given in cm^2/s. Finally, the apparent solubility coefficient, S, can be determined from

$$S = P/D \quad (5)$$

The solubility coefficient is often given in cm^3 (STP)/cm^3 membrane cmHg.

The values at 30 °C of the permeability coefficient of hydrogen, nitrogen, oxygen, carbon dioxide, carbon monoxide, and methane across Poly-HPhNDI membranes, collected in Table 1, follow the trends $P(H_2) > P(CO_2) > P(O_2) > P(CO) > P(CH_4) > P(N_2)$. In the same table, and for comparative purposes, the values of the permeability coefficient of the respective gases through Poly-PhNDI membranes are also shown. In both cases, the permeability coefficients follow similar trends, though their values are significantly higher across the Poly-PhNDI membrane.

Values of the permeability coefficient of the gases across the sulfonated Poly-HPhNDI membrane in the acidic form are shown in Table 2. The results indicate that the ionic groups decrease the permeability coefficient in more than 60%. For example, the value of P for oxygen decreases from 0.66 barrer in Poly-HPhNDI to 0.27 barrer in sulfonated Poly-HPhNDI. Similar behavior also occurs for the other gases.

Results for the diffusion coefficients of the gases in the membranes are shown in Tables 1 and 2. The diffusion coefficient follows the trends $D(H_2) \gg D(O_2) > D(N_2) > D(CO_2) > D(CO) > D(CH_4)$. Whatever the gas considered is, the diffusion coefficient follows the trends D(Poly-PhNDI) > D(Poly-HPhNDI) > D(sulfonated Poly-HPhNDI). Hydrogen exhibits by far the lowest solubility coefficient, the values of this quantity in 10^3 cm^3 (STP)/(cm^3 cmHg) being 0.83, 0.62, and 0.20 respectively in the Poly-PhNDI, Poly-HPhNDI, and sulfonated Poly-HPhNDI membranes. As usual, carbon dioxide presents the highest solubility coefficient; the values of this quantity for the membranes in the order and units indicated above are 63.20, 63.00, and 71.62, respectively.

(B) Electromotive Forces and Conductivity. The electromotive forces (emf) arising from concentration potentials were measured with Ag/AgCl electrodes. To avoid polarization effects on the side of the membranes in contact with the electrolyte solutions, strong stirring was kept during the measurements. Illustrative plots showing the evolution with time of the emf of the membrane for 2 m concentration ratios of hydrochloric acid, $m_2/m_1 = 0.2/0.1$ and 1/0.5, are shown in Figure 2. Since the membrane was equilibrated with water, the emf increases with time, first rather fast and then slowly in such a way that reaching steady-state conditions can take more than 2 h. If prior to the experiment the membrane is equilibrated with the less concentrated hydrochloric acid solution, the time necessary for the emf

Table 1. Values of Permeability (barrer), Diffusion (cm^2/s), and Solubility (cm^3 (STP)/cm^3 of Polymer cmHg) Coefficients for Different Gases at 30 °C and 1 atm of Pressure for Poly-PhNDI and Poly-HPhNDI Membranes

	Poly-PhNDI			Poly-HPhNDI		
gas	P	$D \times 10^9$	$S \times 10^3$	P	$D \times 10^9$	$S \times 10^3$
H_2	11.0	1320.0	0.83	7.22	1164.2	0.62
N_2	0.31	22.3	1.39	0.12	9.4	1.28
O_2	1.44	63.0	2.29	0.66	31.1	2.12
CO_2	11.44	18.1	63.20	4.51	7.2	62.64
CO	0.52	14.5	3.59	0.21	7.6	2.76
CH_4	0.54	7.2	7.50	0.15	1.8	8.33

Table 2. Values of Permeability, *P*, Diffusion, *D*, and Solubility, *S*, Coefficients for Different Gases at 30 °C and 1 atm of Pressure for the Sulfonated Poly-HPhNDI Membrane

gas	P, barrer	$D \times 10^9$, cm^2/s	$S \times 10^3$, cm^3 (STP)/cm^3 cmHg
H_2	4.25	2123.3	0.20
N_2	4.38×10^{-2}	3.2	1.37
O_2	0.27	11.8	2.29
CO_2	1.98	2.8	70.71
CO	8.39×10^{-2}	3.2	2.62
CH_4	4.88×10^{-2}	0.6	8.13

Table 3. Values of the Hydrochloric Acid Concentration (Molality), *m*, Activity Coefficient, γ, and Electromotive Force, emf, for the Sulfonated Poly-HPhNDI Membrane

m_1	m_2	γ_1	γ_2	emf (mV)
5.246×10^{-3}	1.0434×10^{-2}	0.9337	0.9085	34.20
1.0434×10^{-2}	2.0784×10^{-2}	0.9085	0.8830	33.69
5.1956×10^{-2}	0.1037	0.8400	0.8005	31.30
0.1037	0.1977	0.8005	0.7733	29.97
0.1977	0.4113	0.7733	0.7640	28.80
0.4113	0.7757	0.7640	0.7900	25.80
0.5180	0.9996	0.7624	0.8190	40.10

Table 4. Values of the Sodium Chloride Concentration (Molality), Activity Coefficient, and Electromotive Forces for the Sulfonated Poly-HPhNDI Membrane

m_1	m_2	γ_1	γ_2	emf (mV)
0.00472	0.00945	0.9348	0.9081	35.27
0.00945	0.01889	0.785	0.7405	33.43
0.187	0.377	0.7405	0.6860	31.20
0.472	1.001	0.670	0.6362	33.6
0.9897	1.972	0.6292	0.6508	34.10

of the cell to reach steady-state conditions is considerably shortened. On the other hand, only the sign of the emf changes when the concentrations in the compartments flanking the membrane are reversed. This behavior indicates that the cation-exchange membrane is symmetric. Values of the emf of the concentration cells for different m_2/m_1 concentration ratios are shown in Tables 3 and 4 respectively for HCl and NaCl electrolytes. As usual, the values of the emf decrease as the concentration of the electrolyte increases. However, an unexpected result appears in the case of the hydrochloric acid concentration cell: a sharp increase in the emf of the cell is observed when the concentrations flanking the membrane are 0.5/1. This high emf is maintained for values of $m_2/m_1 > 0.5/1$.

The water uptake of the membranes is rather low in spite of the moderately high concentration of fixed ions attached to the chains of the membrane. The protonic resistance, R_0, of the membranes equilibrated with distilled water was measured at 25 °C by impedance spectroscopy. A Bode plot showing the frequency dependence of the modulus of the impedance, $|Z^*|$, for the sulfonated Poly-HPhNDI membrane is shown in Figure 3. As usual, the modulus decreases with increasing frequency, reaching a pseudo-plateau at high frequencies. In Figure 3 the evolution of $\phi = \tan^{-1}(Z''/Z')$ is also shown. It can be seen that

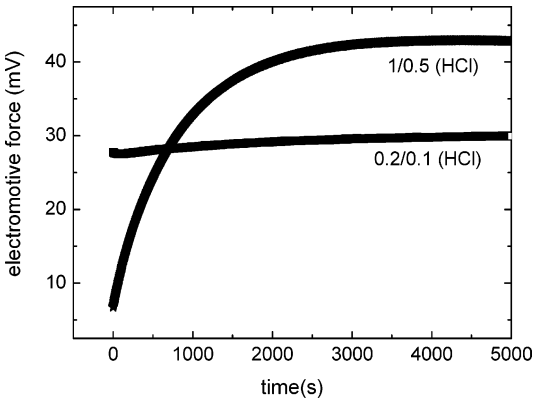

Figure 2. Evolution of the electromotive force of the concentration cell with time. Prior to the experiment, the membrane was equilibrated with water.

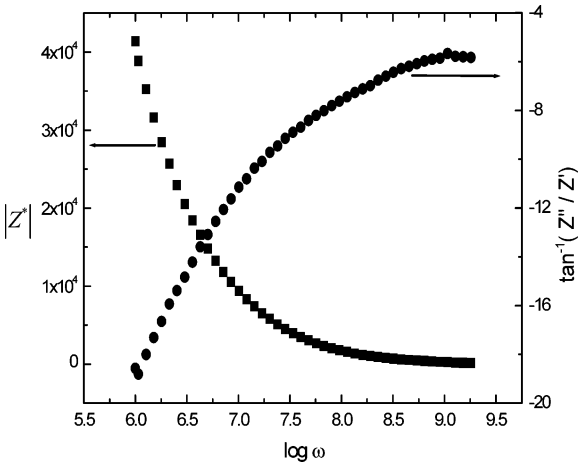

Figure 3. Bode diagram which depicts the evolution of both the modulus of the complex impedance, $|Z^*|$, and the phase angle, $\tan^{-1}(Z''/Z')$, with frequency.

ϕ approaches to a maximum close to zero as frequency increases. The value of $|Z^*|$ at the maximum of the curve ϕ vs $\log f$ was taken as R_0, its value being 147 Ω. Since the diameter and thickness of the sample are 5 and 0.119 mm, respectively, the value of the protonic conductivity, σ, is 4.14×10^{-2} S/m, nearly 2 orders of magnitude below that reported for Nafion membranes.

Discussion

Comparison of the permeation results across the Poly-PhNDI, Poly-HPhNDI, and the sulfonated Poly-HPhNDI membranes shows that hydrogenation of Poly-PhNDI decreases the permeation of the resulting membrane. The results of Tables 1 and 2 suggest that the reduction of the permeation coefficient is not caused by the solubility but by the diffusive step. This behavior suggests that hydrogenation of the double blonds of Poly-PhNDI facilitates chains packaging in Poly-HPhNDI membranes. The free volume diminution caused by the increase of chains packaging efficiency leads to the decrease of the diffusion coefficient. Anchoring fixed sulfonic groups to the chains of Poly-HPhNDI membranes reduces even more gas diffusion across them. This behavior suggests that gas permeation might be lower in the hydrophilic domains than in the hydrophobic domains of the sulfonated Poly-HPhNDI membrane.

The apparent solubility coefficient of the gases in the three membranes is rather similar. It is worth noting that the apparent solubility coefficient of CO_2 in the sulfonated Poly-HPhNDI membrane is slightly higher than in either the Poly-PhNDI or

Table 5. Values of the Enthalpic Interaction Parameter, χ, at 30 °C for Different Gases in the Polynorbornene Membranes

gas	Poly-PhNDI	Poly-HPhNDI	sulfonated Poly-HPhNDI
O_2	+1.05	+1.13	+1.05
N_2	+0.67	+0.77	+0.71
CO_2	−0.18	−0.02	−0.30
CO	+0.23	+0.52	+0.56
CH_4	+0.39	+0.31	+0.34

the Poly-HPhNDI membranes presumably as a consequence of the quadropole nature of the carbon dioxide molecule slightly favoring its interactions with the ionic fixed groups. The pressure dependence of the solubility coefficient of gases in glassy membranes is described by the dual-mode model.[27,28] The model assumes the membranes made up of a continuous phase in which the sorption process follows Henry's law. Microcavities accounting for the excess volume are dispersed in the continuous phase where adsorption processes take place. According to the model, $\lim_{p\to\infty} S = k_D$, where k_D is the Henry's constant, while $\lim_{p\to 0} S = k_D + bC'_H$, where C'_H is the gas concentration adsorbed in the microcavities or Langmuir sites and b is a parameter that accounts for the affinity gas membrane. In most cases a sharp drop in the solubility coefficient at low pressures occurs, this parameter reaching a nearly constant value at pressures in the vicinity of 1 bar. Therefore, k_D was taken as the value of S at 1 bar. Thermodynamics arguments lead to the following expression for Henry's constant[29−31]

$$k_D = \frac{22414}{76V}\exp\left[-(1+\chi) - \frac{\lambda}{RT_b}\left(1 - \frac{T_b}{T}\right)\right] \qquad (6)$$

where $\bar{V}$ is the partial molar volume of the gas in the liquid state, T_b is the boiling temperature of the gas under 1 atm of pressure, χ is the gas in the liquid state−polymer enthalpic interaction parameter, λ is the latent heat of vaporization, R is the gas constant, and T is the absolute temperature of the experiment. Values of χ at 30 °C are given in Table 5. It can be seen that the interaction parameter gas−polymer is similar for Poly-PhNDI, Poly-HPhNDI, and sulfonated Poly-HPhNDI membranes. In all the cases, oxygen exhibits the highest value of χ and CO_2 the lowest. The fact that χ is slightly negative for CO_2 indicates very favorable polymer segments−carbon dioxide interactions.

Usually, membranes permselectivity is defined in terms of the permselectivity coefficient defined as

$$\alpha(A/B) = \frac{P_A}{P_B} = \frac{D_A}{D_B}\frac{S_A}{S_B} \qquad (7)$$

In general, the permselectivity coefficient of pair of gases increases as the permeation of the membranes decreases. For example, the values at 30 °C of $\alpha(O_2/N_2)$ for the Poly-PhNDI, Poly-HPhNDI, and sulfonated PolyHPhNDI membranes are respectively 4.6, 5.5, and 6.1. The fact that the ratios of the diffusion coefficients of the respective gases are respectively 2.8, 3.7, and 3.7 suggests that the diffusion rather than the solubility step is mainly responsible for the permselectivity of the membranes. Therefore, the enhancement of the permselectivity of pairs of low-condensability gases is mainly due to the decrease of diffusion coefficient caused by the augment of the efficiency of molecular packaging. In the case of the permselectivity coefficient of pair of gases in which one of them exhibits high condensability, permselectivity may be not mainly governed by the diffusion coefficient. Thus, $\alpha(CO_2/CH_4)$ for Poly-PhNDI, Poly-HPhNDI, and sulfonated Poly-HPhNDI is 21.2, 30.1, and 40.0 at 30 °C while the values of $D(CO_2/CH_4)$ are 2.5, 4.0, and 4.6, respectively. This means that the increase in permselectivity by effect of the efficiency of molecular packaging is not so large as $D(CO_2/CH_4)$ predicts due to the decrease of the CO_2 solubility as packaging efficiency increases.

The correspondence between electromotive forces of the concentration cells and ionic permselectivity can be obtained from irreversible thermodynamic arguments. Let us consider a concentration cell with configuration Ag|AgCl/electrolyte $A_{\nu_+}B_{\nu_-}$ (m_1)|cation-exchange membrane|electrolyte $A_{\nu_+}B_{\nu_-}$ (m_2)|AgCl/Ag. If the cell is reversible to one of the ionic components of the electrodes, for example to the anion, the electrical potential, $\Delta\psi$, is related to the chemical potential of the anions, $\Delta\mu_-$, by $\Delta\psi = -\Delta\mu_-/z_-F$, where z_- and F are respectively the valence of the anions and Faraday's constant. Fluxes of anions, j_-, cations, j_+, and water, j_w, occur across the membrane under the action of the respective forces: grad μ_-, grad μ_+, and grad μ_w. The production of entropy under unidirectional driving forces can be written as[32]

$$T\dot{s} = j_+\frac{d\mu_+}{dx} + j_-z_-\frac{d\psi}{dx} + j_w\frac{d\mu_w}{dx} \qquad (8)$$

By taking into account the neutrality principle ($\nu_+z_+ + \nu_-z_- = 0$), the chemical potential of the electrolyte ($\mu_s = \nu_+\mu_+ + \nu_-\mu_-$) and the Gibbs−Duhem relation ($m_+\nu_+ d\mu_+ + m_-\nu_- d\mu_- + m_w d\mu_w = 0$), where m_k represents the molality of the k particle, eq 8 becomes[33]

$$-T\dot{s} = \frac{1}{\nu_+}j_+^1\frac{d\mu_2}{dx} + i\frac{d\psi}{dx} \qquad (9)$$

where $j_+^1 = j_+ - (\nu_+m_2/c_w)j_w$ is the counterion flux taking the moving liquid in the membrane as reference frame. The parameter $i = F(z_+j_+ + z_-j_-)$ is the electrical current flux. Hence, the fluxes are j_+^1/ν_+ and i whereas the forces are $d\mu_2/dx$ and $d\psi/dx$. Taking into account that the fluxes are linear function of the forces, then

$$\frac{j_+^1}{\nu_+} = \lambda_{11}\frac{d\mu_2}{dx} + \lambda_{12}\frac{d\psi}{dx} \qquad (10)$$

$$i = \lambda_{21}\frac{d\mu_2}{dx} + \lambda_{22}\frac{d\psi}{dx} \qquad (11)$$

where λ_{kl} ($k, l = 1, 2$) are the Onsager coefficients. It is easy to show from eqs 10 and 11 respectively that $\lambda_{11} = -D_2^1$ (ψ = const) and $\lambda_{22} = i/(d\psi/dx) = -\sigma$ (μ_2 = const), where σ is the conductivity. Let us consider in more detail the coefficient $\lambda_{12} = \lambda_{21}$. Taking as reference frame the moving liquid, the counterion transport number is $t_+^1 = z_+j_+^1/Fi$. Then for μ_2 = const, eq 11 leads to $\lambda_{12} = \lambda_{21} = -(t_+^1\sigma/\nu_+z_+F)$, where F is Faraday's constant. Accordingly, the electric potential gradient can be obtained from eq 11 yielding

$$\frac{d\psi}{dx} = -\frac{i}{\sigma} - \frac{t_+^1}{\nu_+z_+F}\frac{d\mu_2}{dx} \qquad (12)$$

During the electromotive force measurements $i = 0$, and in this situation eq 12 leads to the following expression for the electromotive force E of the concentration cell

$$E = \Delta\psi = -\frac{RT\nu_2}{z_+\nu_+F}\int_{a_2^1}^{a_2^2} t_+^1\, d\ln a_2 \qquad (13)$$

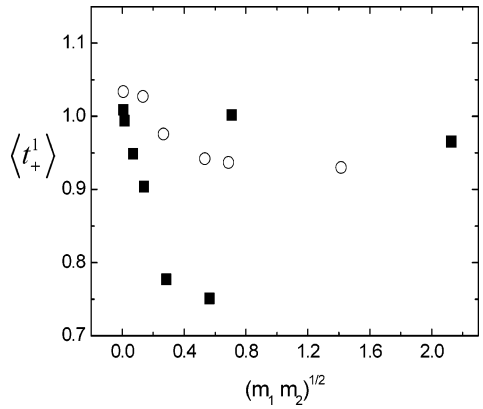

Figure 4. Variation of the apparent proton (squares) and sodium cation (circles) transport numbers with the geometric average of the HCl and NaCl solutions flanking the membrane.

where $a_2^1$and a_2^2 represent respectively the activities of the low and high concentration electrolyte solutions flanking the membranes and $\nu_2 = \nu_+ + \nu_-$. Although the counterion transport number depends on concentration, an average value of this parameter can be obtained from the expression

$$\langle t_+^1 \rangle = E/E_{\max} \tag{14}$$

where $E_{\max}$ is the electromotive force for an ideally permselective membrane obtained from eq 13 doing $t_+^1 = 1$.

Let us consider first the transport number of protons across the membrane flanked by electrolyte solutions of different concentration. Values of the transport number-average for protons in the range $m_2/m_1 = 0.01/0.005$ to $m_2/m_1 = 2/1$, where m is the molality of the hydrochloric acid solutions, are plotted as a function of $\bar{m} = (m_1 m_2)^{1/2}$ in Figure 4. It can be seen that for very low values of $\bar{m}$ the membrane is ideally permselective to protons, that is, $\langle t_+^1 \rangle = 1$. This behavior is a consequence of the fact that co-ions are totally excluded from the membrane at very low concentrations so that current is exclusively transported across the membrane by protons. At moderate and high concentrations, however, free hydrochloric acid diffuses into the membrane as $\bar{m}$ increases, and as a result co-ions intervene in the current transport across the membrane. In this situation, $\langle t_-^1 \rangle > 0$, and taking into account that $\langle t_+^1 \rangle + \langle t_-^1 \rangle = 1$, then $\langle t_+^1 \rangle < 1$. The values of the transport number for protons decrease as the concentration increases. However, at rather high concentrations a sharp increase in the value of $\langle t_+^1 \rangle$ takes place, and the membrane behaves as nearly ideally permselective again. At first glance, one would expect some sort of protonation of the imide groups by the high concentrated hydrochloric acid that would give rise to the introduction of positive fixed groups in the membrane, converting it into an amphoteric one. This process would enhance the transport of current across the membrane by co-ions, but this does not seem to be the case because $\langle t_+^1 \rangle \cong 1$. Therefore, the only way of interpreting the experimental results is to postulate that co-ions presumably form some sort of pair ions with protonated imide groups that restrict their mobility across the membranes. Further research involving NMR spectroscopy is necessary to clarify this apparently anomalous result.

As can be seen in Figure 5, the permselectivity of the membranes to sodium ions follows similar trends as that found for protons. At very low concentrations the transport number of sodium cations lies in the vicinity of 1, the membrane behaving as ideally selectivity. As usual, the transport number decreases with increasing concentration of the sodium chloride in the solutions of the concentration cell. In this region, the transport number of Na^+ is slightly lower than that of H^+. However, at very high concentrations the transport number of Na^+ is still rather high, but the anomalous concentration dependence observed for protons is not detected here.

There is a vivid debate concerning both the nature of the water in wet ion-exchange membranes and the proton transport mechanism.[34] The information at hand, corroborated by structural simulations of the membranes phase, suggests that water and protons are confined to domains of only nanometers, and proton conduction would be carried out in the domains through a percolation path. Recent simulations carried out on the proton conductivity in sulfonic polyphenyl sulfone membranes suggests that hydrated protons, H_3O^+, rather than naked protons, H^+, intervene in the process.[35] The sulfonated Poly-HPhNDI membranes used in this study exhibit a moderate conductivity if their low water uptake (12.4%) is considered. It seems that the segregation between hydrophilic domains containing ionic fixed water and counterions from the hydrophobic domains that hinder ionic diffusion across them. It can be shown that the proton conductivity, σ, is related to the free diffusion, D_+, by[35,36]

$$\sigma = \frac{c_+ F^2 D_+}{RT} \tag{15}$$

where c_+ is the concentration of protons in the membrane phase, F is the Faraday's constant, and RT has the usual meaning. In membranes equilibrated with water, the concentration of protons in the membrane is equal to the concentration of fixed groups, which in this case is 0.82 mequiv/g of dry membrane. Since the density of the wet membrane is 1.1 g/cm^3, and taking into account that $\sigma = 4.14 \times 10^{-2}$ S/m, the diffusion coefficient of protons is about 1.5×10^{-7} cm^2/s. The rather low value of D_+ suggests that the percolation path across the hydrophilic domains may be interrupted by hydrophobic domains which control the diffusion step. It is possible that protons diffuse in hydrophilic microdomains until fluctuations in the hydrophobic microdomains may form channels through which protons slide to a nearby hydrophilic domain.

Conclusions

Hydrogenation of membranes based on polynorbornenes functionalized with imide side groups reduces gas permeability across them as a consequence of the increase of packaging efficiency of the molecular chains. The permeability is even lower in the membranes with fixed negative groups anchored to their structure. The reduction in gas permeation is accompanied by an increase in gas permselectivity.

Sulfonated membranes exhibit a high cationic permselectivity at low electrolyte concentrations. Permselectivity of the membranes to protons decreases with increasing concentration until a concentration is reached at which a sharp increase in permselectivy is observed. This behavior suggests some sort of pair ions formation between protonated imide groups and Cl^- that reduces co-ions mobility. Further research involving NMR spectroscopy is necessary to clarify this issue.

The rather low value of D_+ suggests that fluctuations of the molecular chains of the hydrophobic domains may form channels through which protons slide to a nearby hydrophilic domain. These channels will control the protonic conductivity of the sulfonated Poly-HPhNDI membranes.

Acknowledgment. We thank Dr. T. Ezquerra (Instituto de Estructura de la Materia, CSIC) for the membranes conductivity

measurements. This work was supported by the Comunidad de Madrid (CAM) through the Program Interfases (S-0505/MAT-0227), Fondo Europeo de Desarrollo Regional (F.E.D-.E.R.), and Fondo Social Europeo (F.S.E.). Support by the Dirección General de Investigación Científica y Técnica (DGICYT), Grant MAT-2005-05648-C02-01, is gratefully acknowledged.

References and Notes

(1) Kesting, R. E.; Fritzsche, A. K. *Polymer Gas Separation Membranes*; Wiley-Interscience: New York, 1993.
(2) *Polymer Membranes for Gas and Vapor Separation: Chemistry and Materials Science*; Freeman, B. D., Pinnau, I., Eds.; American Chemical Society: Washington, DC, 1999.
(3) Ivin, K. J.; Mol, J. C. In *Olefin Methathesis and Methathesis Polymerization*; Academic Press: San Diego, CA, 1997; Chapter 13. Tlenkopatchev, M. A.; Fomine, S.; Fomina, L.; Gaviño, R.; Ogawa, T. *Polym. J.* **1997**, *29*, 622.
(4) Maya, V. G.; Contreras, A. P.; Canseco, M.-A.; Tlenkopatchev, M. A. *React. Funct. Polym.* **2001**, *49*, 145.
(5) Paul, D. R.; Yampolskii, Yu. P. *Polymeric Gas Separation Membranes*; CRC Press: Boca Raton, FL, 1994.
(6) Bondar, V. I.; Kukharskiii, Yu.; Yampolskii, Yu. P. M.; Finkelshtein, E. Sh.; Makovetskii, K. L. *J. Polym. Sci., Part B: Polym. Phys.* **1993**, *31*, 1273.
(7) Yampolskii, Yu. P.; Bespalova, N. B.; Finkelshtein, E. Sh.; Makovetskii, K. L.; Bondar, V. I.; Popov, A. V. *Macromolecules* **1994**, *27*, 2872.
(8) Yampolskii, Yu. P.; Finkelshtein, E. Sh.; Makovetskii, K. L.; Bondar, V. I.; Shantarovich, V. P. *J. Appl. Polym. Sci.* **1996**, *62*, 349.
(9) Dorkenoo, K. D.; Pfromm, P. H.; Rezak, M. E. *J. Polym. Sci., Part B: Polym. Phys.* **1998**, *36*, 797.
(10) Zhao, Ch-T.; Do Rosario Ribeiro, M.; de Pinho, M. N.; Subrahmanyan, V. S.; Gil, C. L.; de Lima, A. P. *Polymer* **2001**, *42*, 2455.
(11) Contreras, A. P.; Tlenkopatchev, M. A.; Ogawa, T.; Nakagawa, T. *Polym. J.* **2002**, *34*, 49.
(12) Pineda-Contreras, A.; Tlenkopatchev, M. A.; López-González, M.; Riande, E. *Macromolecules* **2002**, *35*, 4677.
(13) Tlenkopatchev, M. A.; Vargas, J.; López-González, M. M.; Riande, E. *Macromolecules* **2003**, *36*, 8483.
(14) Díaz, K.; Vargas, J.; del Castillo, L. F.; Tlenkopatchev, M. A.; Aguilar-Vega, M. *Macromol. Chem. Phys.* **2005**, *206*, 2316.
(15) Hickner, M. A.; Gashomi, H.; Kim, Y. S.; Einsla, B. R.; McGrath, E. *Chem. Rev.* **2004**, *104*, 4587.
(16) Kruczek, B.; Matsuura, T. *J. Membr. Sci.* **1998**, *146*, 263.
(17) Hu, W.; Adachi, K.; Matsumoto, H.; Tanioka, A. *J. Chem. Soc., Faraday Trans.* **1998**, *94*, 665.
(18) Sungpet, A.; Way, J. D.; Thoen, P. M.; Dorgan, J. R. *J. Membr. Sci.* **1997**, *136*, 111.
(19) Yamaguchi, T.; Koval, C. A.; Noble, R. D.; Bowman, C. N. *Chem. Eng. Sci.* **1996**, *51*, 4781.
(20) Boyd, T. H.; Schrock, R. R. *Macromolecules* **1999**, *32*, 6608.
(21) Fernandez-Carretero, F. J.; Compañ, V.; Riande, E.; Linares, A.; Acosta, J. L. *J. Electrochem. Soc.*, in press.
(22) Asrar, J. *Macromolecules* **1992**, *25*, 5150.
(23) Elabad, Y. A.; Napadensky, E. *Polymer* **2004**, *45*, 3037.
(24) Ezquerra, T. A.; Kremer, J.; Wegner, G. Progress in Electromagnetic Research. In *Dielectric Properties of Heterogeneous Materials*; Priou, A., Ed.; Elsevier: Amsterdam, 1992; Vol. 6.
(25) Bode, W. W. *Network Analysis and Feedback Amplifier Design*; Van Nostrand: Princeton, NJ, 1956.
(26) Barrer, R. M. *Trans. Faraday Soc.* **1939**, *35*, 628.
(27) Vieth, W. R.; Sladek, K. J. *J. Colloid Sci.* **1965**, 20 1014.
(28) Ohya, H.; Kudryavtsev, V. V.; Semenova, S. J. *Polyimide Membranes*; Gordon and Breach Publishers: Tokyo, 1996; p 60.
(29) Petropoulos, J. H. *Pure Appl. Chem.* **1993**, *65*, 219.
(30) Compañ, V.; López-González, M. M.; Riande, E. *Macromolecules* **2003**, *36*, 8576.
(31) Tlenkopatchev, M. A.; Vargas, J.; Girón, M. A.; López González, M.; Riande, E. *Macromolecules* **2005**, *38*, 2696.
(32) Haase, R. *Thermodynamics of Irreversible Processes*, 2nd ed.; Dover: New York, 1990.
(33) López, M. L.; Compañ, V.; Garrido, J.; Riande, E.; Acosta, J. L. *J. Electrochem. Soc.* **2001**, *148*, E372.
(34) Paddison, S. J. *Annu. Rev. Mater. Res.* **2003**, *33*, 289.
(35) Pozuelo, J.; Riande, E.; Saiz, E.; Compañ, V. *Macromolecules* **2006**, *39*, 8862.
(36) Sata, T. *Ion-Exchange Membranes*; Royal Society of Chemistry: Cambridge, 2004; Chapter 1.

MA062522Q